Evidence for a *gem*-Diol Reaction Intermediate in Bacterial C−C Hydrolase Enzymes BphD and MhpC from ^{13}C NMR Spectroscopy†

Jian-Jun Li, Chen Li, Claudia A. Blindauer, and Timothy D. H. Bugg*

Department of Chemistry, University of Warwick, Coventry CV4 7AL, U.K.

Received June 23, 2006; Revised Manuscript Received August 15, 2006

ABSTRACT: C−C hydrolase enzymes MhpC and BphD catalyze the hydrolytic C−C cleavage of *meta*-ring fission intermediates on the *Escherichia coli* phenylpropionic acid and *Burkholderia xenovorans* LB400 biphenyl degradation pathways and are both members of the α/β-hydrolase family containing a Ser-His-Asp catalytic triad. The catalytic mechanism of this family of enzymes is thought to proceed via a *gem*-diol reaction intermediate, which has not been observed directly. Site-directed single mutants of BphD in which catalytic residues His-265 and Ser-112 were replaced with Ala were found to possess 10^4-fold reduced k_{cat} values, and in each case, the C−C cleavage step was shown by pre-steady-state kinetic analysis to be rate-limiting. The processing of a 6-^{13}C-labeled aryl-containing substrate by these H265A or S112A mutant BphD enzymes was monitored directly by ^{13}C NMR spectroscopy. A new line-broadened signal was observed at 128 ppm for each enzyme, corresponding to the proposed *gem*-diol reaction intermediate, over a time scale of 1−24 h. A similar signal was observed upon incubation of the ^{13}C-labeled substrate with an H114A MhpC mutant, which is able to accept the 6-phenyl-containing substrate, on a shorter time scale. The direct observation of a *gem*-diol intermediate provides further evidence that supports a general base mechanism for this family of enzymes.

The α/β-hydrolase superfamily of enzymes, comprised mainly of lipase and esterase enzymes, contains a Ser-His-Asp catalytic triad (*1*). The role of the active site serine residue is believed to be, as in the archetypal serine proteases, that of a nucleophile, which attacks the carbonyl group of the substrate to form an oxyanion intermediate and an ensuing acyl−enzyme intermediate (*2*). The α/β-hydrolase superfamily also contains a diverse range of other catalytic activities (*1*, *3*), including a family of C−C hydrolase enzymes found on bacterial *meta*-cleavage pathways, where they catalyze the hydrolytic cleavage of dienol ring fission product **1** (RFP)[1] (*4*). Investigations of the catalytic mechanism of *Escherichia coli* C−C hydrolase MhpC have shown that the reaction proceeds via an initial keto−enol tautomerization, to give a keto intermediate **2** (RFP^k), followed by C−C cleavage (*5*, *6*). Surprisingly, further studies showed that a covalent acyl enzyme (**3**) could not be observed by radiochemical trapping methods (*7*). Moreover, the observation of MhpC-catalyzed exchange of ^{18}O at the substrate carbonyl (*7*) and the turnover of a reduced substrate analogue by the related C−C hydrolase BphD from *Burkholderia xenovorans* LB400 (*8*) are consistent with a general base mechanism proceeding via a *gem*-diol intermediate (**4**), as shown in Figure 1.

Structural information is available for three C−C hydrolase enzymes in this family: ligand-free structures of BphD from *Rhodococcus* sp. RHA1 (*9*) and CumD from *Pseudomonas fluorescens* (*10*) and the structure of *E. coli* MhpC complexed with a noncleavable substrate analogue, 2,6-diketonona-1,9-dioic acid (*11*). The MhpC structure indicated that catalytic residues His-263 and Ser-110 straddle the bound substrate analogue and identified active site residues Arg-188, His-114, and Ser-40 close to the bound substrate analogue (*11*). Replacement of Ser-110 or His-263 of MhpC with Ala gave mutant enzymes with 10^4-fold reduced k_{cat} values but with a low level of activity for C−C cleavage (*12*).

C−C hydrolase BphD from *B. xenovorans* LB400 bears 50% sequence identity to *E. coli* MhpC and accepts an aryl-containing ring fission intermediate on the biphenyl degradation pathway (*13*). We have developed a chemical synthesis of the aryl-containing *meta*-ring fission products (*8*), which we have used to measure a Hammett plot for processing of *para*-substituted aryl substrates by BphD (*14*) and to determine the stereochemical course of the BphD-catalyzed reaction (*15*). In this paper, we describe the enzymatic processing of a specifically ^{13}C-labeled substrate, containing ^{13}C at the C-6 carbonyl group. If the enzyme-bound intermediate(s) can be observed directly by ^{13}C NMR spectroscopy, then this labeled substrate can be used unambiguously to distinguish a *gem*-diol intermediate **4** (δ_C 100−130) from an acyl−enzyme intermediate **3** (δ_C 170−175), as illustrated in Figure 1.

† This work was supported by BBSRC (Grant B20467), the University of Warwick, the Royal Society (Olga Kennard Fellowship to C.A.B.), and ORS.

* To whom correspondence should be addressed. Telephone: 02476-573018. Fax: 02476-524112. E-mail: T.D.Bugg@warwick.ac.uk.

[1] Abbreviations: MhpC, 2-hydroxy-6-ketonona-2,4-diene-1,9-dioic acid 5,6-hydrolase; BphD, 2-hydroxy-6-keto-6-phenylhexa-2,4-dienoic acid 5,6-hydrolase; RFP, ring fission product (**1**); HPD, 2-hydroxypentadienoic acid; NMR, nuclear magnetic resonance; ES-MS, electrospray mass spectrometry; IPTG, β-isopropyl thiogalactoside; SDS−PAGE, sodium dodecyl sulfate−polyacrylamide gel electrophoresis.

10.1021/bi0612519 CCC: $33.50
Published on Web 09/21/2006

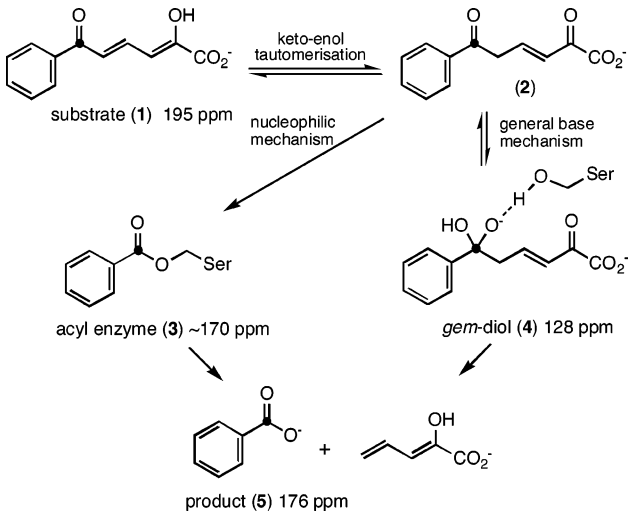

FIGURE 1: Reaction catalyzed by C−C hydrolase BphD, showing general base and nucleophilic mechanisms. The position of the ^{13}C label and the expected/observed chemical shifts are given for each species.

MATERIALS AND METHODS

Materials. Restriction enzymes were obtained from Fermentas Life Sciences. T4 DNA ligase was from New England Biolabs. The QuickChange site-directed mutagenesis kit was from Stratagene. IPTG was purchased from Melford Laboratories Ltd. Vector pET-14b was from Merck Biosciences. All other chemicals and biochemicals were purchased from Sigma or Aldrich.

Synthesis of 6-^{13}C-Labeled Substrate and Unlabeled Substrate. The synthetic route of Speare et al. was used, via reaction of [1-^{13}C]benzaldehyde (>99% ^{13}C, Aldrich) with vinyl magnesium bromide, followed by a Heck coupling reaction (*8*). The intermediate [6-^{13}C]ethyl-2-acetoxy-6-keto-6-phenylhexa-2,4-dienoate (*8*), isolated in 16% overall yield (80 mg), exhibited ^{1}H NMR data identical to those of unlabeled material: δ_C (75 MHz, $CDCl_3$) 189.3 ppm; *m*/*z* 312.2 (ES-MS, MNa^+, predicted 312.1). The 6-^{13}C-labeled substrate was prepared by alkaline hydrolysis of the diester, as previously described (*8*): δ_C (75 MHz, D_2O) 194.5 ppm; *m*/*z* 258.2 (ES-MS, MK^+, predicted 258.1). Unlabeled substrate was synthesized using the same procedure (*8*).

Construction of Site-Directed Mutants. The *B. xenovorans* LB400 *bphD* gene was amplified by polymerase chain reaction and cloned into the pET-14b vector, using restriction enzymes *Bam*HI and *Nde*I. The construct pET14b-BphD was used for high-level expression of the His_6-tagged BphD fusion protein. Mutants S112A and D237N were created by the method of splicing by overlap extension (*26*), using the primers listed in Table 1. Mutant H265A was created according to the QuickChange site-directed mutagenesis protocol. The required mutations were confirmed by DNA sequencing. The MhpC mutant H114A was constructed as previously described (*12*).

Expression and Purification of Wild-Type BphD and Mutants. BL21(DE3) host cells were transformed with wild-type pET14b-BphD or mutant constructs. Overexpression of BphD was induced with 75 μM IPTG at 16 °C, followed by growth for 2 days at this temperature. The cells were collected by centrifugation for 10 min at 5000*g* and resuspended in 40 mL of buffer A [50 mM sodium phosphate buffer (pH 8.0) containing 0.3 M sodium chloride]. Cell lysis was conducted by sonication, followed by centrifugation for 25 min at 12000*g*. The supernatant was loaded onto a Talon metal affinity column (BD Biosciences Clontech, 2.5 cm × 4 cm) and eluted at flow rate 1.0 mL/min with 100 mL of buffer A, followed by a linear 0 to 0.2 M imidazole gradient [100 mL of buffer A and 100 mL of buffer B (buffer A with 0.2 M imidazole)]. BphD was eluted from the column at 80 μM imidazole. The enzyme purity was analyzed via 12% SDS−PAGE. The fractions containing BphD were pooled. The protein concentration was determined by the Bradford method using bovine serum albumin as a standard. The yield of wild-type BphD was 30 mg, with a specific activity of 11.8 units/mg, from a 2 L culture. The yields of BphD mutants H265A and S112A were 50 and 35 mg, respectively, from 2 L cultures. MhpC mutant H114A was expressed and purified as previously described (*12*). Each enzyme was estimated to be >90% pure by SDS−PAGE.

Steady-State Kinetic Measurements. The substrate was prepared as follows. First, 0.5 mL of 0.1 M sodium hydroxide was added to a solution of 3 mg of ethyl-2-acetoxy-6-keto-6-phenylhexa-2,4-dienoate (*8*) in 1 mL of methanol, and then the mixture was stirred for 2 h at room temperature and diluted with 8 mL of 50 mM potassium phosphate buffer (pH 8.0). Then methanol was removed under reduced pressure, and the substrate was used immediately.

The activity of purified wild-type BphD and mutants was assayed by monitoring the decrease in absorbance at 434 nm due to the consumption of the substrate ($\epsilon = 26\,300\ M^{-1}\ cm^{-1}$ at pH 8.0) on a Cary 1 UV−vis spectrophotometer at 25 °C. Assays were carried out in 50 mM potassium phosphate buffer (pH 8.0) in a 1.0 mL volume. K_M was determined in duplicate, using Lineweaver−Burk plots. k_{cat} was calculated from the maximum specific activity of the purified enzyme on the basis of catalytic efficiency per 33 kDa subunit.

Pre-Steady-State Kinetic Measurements. The pre-steady-state kinetic assays on wild-type BphD and mutants S112A, H265A, D237N, H265A, and H114A MhpC were carried out using a DX.17MV stopped-flow spectrometer (Applied Photophysics Ltd.). The enzymes and substrate were in 50 mM potassium phosphate buffer (pH 7.0). In each stopped-flow experiment, solutions of 1 mg/mL enzyme and 30.3 M substrate ([E]:[S] = 1:1) were mixed rapidly in the reaction chamber at room temperature. Disappearance of the substrate was monitored at both 434 nm (substrate dienolate form) and 341 nm (substrate dienol form). The appearance of product HPD was monitored at 270 nm. Data for every shot were simulated with single-, double-, or treble-exponential kinetic models, and the best-fit rate constants and amplitudes were recorded.

^{13}C NMR Spectroscopy. ^{1}H-decoupled ^{13}C NMR spectra were acquired on a Bruker DRX 500 MHz spectrometer fitted with a dual cryoprobe operating at 125.74 MHz for ^{13}C, using a 3.05 μs (30°) excitation pulse, a 1 s recycle delay, a spectral width of 34 kHz, and 64K data points; 32−256 scans were acquired for each spectrum. Raw data were zero-filled to 256K and apodized by exponential multiplication using a line-broadening factor of 15 Hz prior to Fourier transformation. Half-height line widths for narrow resonances were measured on nonapodized spectra. Chemical shifts are reported relative to tetramethylsilane at 0.00 ppm.

Table 1: PCR Primers Used for Site-Directed Mutagenesis of *bphD* Genes

	direction	primer sequence
wild type	forward	5′-GCTCGACATATGACCGCACTCACCGAAAGTTC-3′
	reverse	5′-GTACGTGGATCCTTACGCGTGCCGCAGGAAGT-3′
S112A	forward	5′-ACCTGGTCGGCAAGCGATGGG-3′
	reverse	5′-CCCATCGCGTTGCCGACCAGGTG-3′
H265A	forward	5′-TTTCTCCAAGTGCGGCGCTTGGGCGCAATG-3′
	reverse	5′-ATTGCGCCCAAGCGCCGCACTTGGAG-3′
D237N	forward	5′-GGGCGCGATAATCGCTTCGTTTCC-3′
	reverse	5′-GGAACGAAGCGATTATCGCGCCC-3′

Each experiment was carried out in a total volume of 0.7 mL, in aqueous buffer containing 10% D_2O. The purified mutant enzyme was preconcentrated to a final concentration of 1.0 mM in 50 mM potassium phosphate buffer (pH 7.0) by ultrafiltration. To 560 μL of an enzyme solution was added 70 μL of D_2O, and a control ^{13}C spectrum of enzyme only was recorded. An aliquot of 70 μL of ^{13}C-labeled substrate [100 mM stock in 50 mM potassium phosphate buffer (pH 7.0)] was added, and ^{13}C NMR spectra were recorded thereafter over 64 (4.5 min), 128 (9 min), or 256 scans (18 min). A substrate-only control spectrum was also recorded, after dissolving fresh substrate in buffer.

For the control experiment illustrated in Figure 6, 1.0 mM H114A mutant MhpC was mixed with 2.0 mM ^{13}C-labeled substrate. After 20 min, a further 100 μL aliquot of unlabeled substrate (60 mM stock) was added, and spectra were recorded over 1 h, and after 24 h at 293 K.

Analysis of Substrate Decomposition. Decomposition of substrate (33 μM) in 50 mM potassium phosphate buffer (pH 7.0) was monitored directly at 434 nm for 3 h at 25 °C. On a larger scale, decomposition of the substrate (3 mg) in 50 mM potassium phosphate buffer (pH 7.0, 5.0 mL) was monitored by withdrawal of aliquots at intervals of 5, 10, and 30 min, and injection onto a C_{18} reverse phase column, followed by elution with water at a flow rate of 0.5 mL/min. LC−MS was carried out under the same conditions using an HCTplus mass spectrometer (Bruker). The incubation was left overnight at room temperature, and then the mixture was extracted with ethyl acetate (3 × 20 mL), dried ($MgSO_4$), and evaporated under reduced pressure. The residue was analyzed by ^1H NMR spectroscopy.

RESULTS

Synthesis of 6-^{13}C-Labeled Substrate for BphD. Using the previously developed synthetic route to the BphD substrate 2-hydroxy-6-keto-6-phenylhexa-2,4-dienoic acid (*8*), a specifically 6-^{13}C-labeled substrate was synthesized in 16% overall yield from [1-^{13}C]benzaldehyde. The ^{13}C spectrum of the freshly prepared 6-^{13}C-labeled substrate showed a single peak at 194.5 ppm, corresponding to the C-6 carbonyl group.

Construction and Expression of Wild-Type BphD and Site-Directed BphD Mutants. The *B. xenovorans* LB400 *bphD* gene was cloned into pET14b, to give expression construct pET14b-BphD, from which N-His_6-BphD could be expressed to a high level in *E. coli* BL21(DE3). Three single site-directed BphD mutants were constructed using either splicing by overlap extension or the QuikChange (Stratagene) method. Ser-112 was replaced with Ala, Asp-237 with Asn, and His-265 with Ala. Wild-type BphD and mutants were overexpressed as N-His_6 fusion proteins, allowing rapid purification of enzymes by cobalt-Talon chromatography to >90% homogeneity. It was found that the wild-type N-His_6-BphD fusion protein had a turnover number (k_{cat} = 6.5 s^{-1}; K_M = 2.0 μM) similar to that of native BphD (k_{cat} = 5.0 s^{-1}; K_M = 0.25 μM) but a higher K_M (*13*). The activity of mutant enzymes was determined as their N-His_6 fusions.

Table 2: Steady-State Kinetic Parameters for Wild-Type and Mutant Enzymes[a]

enzyme	K_M (μM)	k_{cat} (s^{-1})	k_{cat}/K_M (M^{-1} s^{-1})
His_6-BphD	2.0	6.5	3.25×10^6
S112A BphD	37.3	0.0009	24.3
H265A BphD	37.0	0.0016	43.2
D237N BphD	1.7	0.028	1.65×10^3
H114A MhpC	23.8	0.036	1.51×10^3

[a] K_M and k_{cat} were determined in 50 mM potassium phosphate buffer (pH 8.0) at 25 °C (±10% error).

Steady-State Kinetic Analysis. Parameters for steady-state kinetics were obtained for each mutant using the natural substrate, in 50 mM potassium phosphate buffer (pH 8.0), as shown in Table 2. Compared with the wild-type enzyme, mutants S112A and H265A exhibited 4000−7000-fold reduced k_{cat} values and 18-fold increased K_M values. The effects upon k_{cat} are comparable to the effects of the same mutations upon *E. coli* MhpC (*12*). D237N exhibited a 200-fold reduced k_{cat} compared with that of the wild type but nearly the same K_M as the wild type. The pH−rate profile for wild-type BphD (data not shown) exhibited maximal activity at pH 6−8, with inflections at pH 5.8 and 8.8, similar to that previously determined for *E. coli* MhpC (*12*).

Pre-Steady-State Kinetic Analysis of Wild-Type BphD and Mutants. Each enzyme was analyzed under single-turnover conditions by stopped-flow UV−visible spectrophotometry in 50 mM potassium phosphate (pH 7.0) at 434 nm (substrate dienolate form), 341 nm (substrate dienol form), and 270 nm (product HPD). The best fit kinetic data are given in Table 3. For wild-type BphD, the data obtained at 341 nm were best simulated by a double-exponential equation, implying a two-step process, with a fast ketonization step (k_1 = 338 s^{-1}) followed by C−C cleavage (k_2 = 14.7 s^{-1}).

Stopped-flow data for BphD mutant S112A at 341 nm could be modeled with a treble-exponential equation, interpreted as a fast ketonization step (k_1 = 367 s^{-1}), followed by slow C−C cleavage (k_2 = 0.04 s^{-1}) and product release (k_3 = 0.006 s^{-1}) steps. The observation that the keto−enol tautomerization step is unaffected by replacement of the catalytic serine residue is similar to what was observed previously for C−C hydrolase MhpC (*12*).

The data recorded for mutant H265A at 434 nm could be modeled with a treble-exponential equation, indicating a three-step process. The first step showed an increase in A_{434}, implying that this step corresponds to the initial dienol-to-

Table 3: Pre-Steady-State Kinetic Parameters for Wild-Type BphD, BphD Mutants, and the MhpC Mutant[a]

	A_1 ($\times 10^3$)	k_1 (s^{-1})	A_2 ($\times 10^3$)	k_2 (s^{-1})	A_3 ($\times 10^3$)	k_3 (s^{-1})
at 434 nm						
wild type	32.2 ± 0.5	220.1 ± 5.6	65.5 ± 0.3	21.3 ± 0.1		
S112A	26.9 ± 0.3	304 ± 7	24.3 ± 0.3	0.03 ± 0.001	28.0 ± 0.3	0.004 ± 0.0001
H265A	-16.9 ± 0.1	1.3 ± 0.02	73.3 ± 0.2	0.016 ± 0.0001	5.3 ± 0.1	0.002 ± 0.0001
D237N	-5.5 ± 0.08	2.6 ± 0.08	44.1 ± 4.8	0.04 ± 0.002	63.2 ± 4.9	0.02 ± 0.001
H114A MhpC	52.2 ± 0.2	0.023 ± 0.0005	86 ± 1	0.0022[b]		
at 341 nm						
wild type	20.0 ± 0.6	338 ± 13	9.1 ± 0.1	14.7 ± 0.3		
S112A	16.0 ± 0.5	367 ± 16	5.6 ± 0.3	0.04 ± 0.003	5.7 ± 0.2	0.006 ± 0.0005
H265A	16.5 ± 0.1	0.014 ± 0.0002	2.8 ± 0.1	0.013 ± 0.0008		
D237N	4.2 ± 0.2	0.03 ± 0.002	3.8 ± 0.2	0.03 ± 0.002		
H114A MhpC	23.5 ± 0.4	0.025 ± 0.0003	15 ± 3	0.004[b]		
at 270 nm[c]						
wild type	-40.5 ± 0.3	32.7 ± 0.4				
S112A	-19.9 ± 0.2	0.08 ± 0.002				
H265A	-41.1 ± 0.3	0.02 ± 0.001				
D237N	-1.4 ± 0.1	0.9 ± 0.2				

[a] Stopped-flow data were obtained in 50 mM potassium phosphate buffer (pH 7.0) at room temperature. Substrate consumption was monitored at both 434 nm (dienolate form of the substrate) and 341 nm (dienol form of the substrate), and product appearance was followed at 270 nm. [b] The second step observed for the MhpC H114A mutant is slower than k_{cat} (0.036 s^{-1}) and is therefore not interpreted to be part of the catalytic cycle. [c] Interpretation of the data recorded for BphD mutants at 270 nm is complicated by the overlapping absorbance of product HPD with the second product, benzoic acid, at this wavelength.

dienolate deprotonation ($k_1 = 1.3\ s^{-1}$), as observed previously in mutant S40A of C−C hydrolase MhpC (*12*). The subsequent ketonization ($k_2 = 0.016\ s^{-1}$) and C−C cleavage ($k_3 = 0.002\ s^{-1}$) steps are both slow, indicating that His-265 is involved in both steps. The data recorded at 341 nm do not show this initial increase step. The data recorded for mutant D237N at 434 nm were similar to those obtained for mutant H265A. Three steps were observed, corresponding to substrate deprotonation ($k_1 = 2.6\ s^{-1}$), ketonization ($k_2 = 0.04\ s^{-1}$), and C−C cleavage ($k_3 = 0.02\ s^{-1}$).

Processing of 6-^{13}C-Labeled Substrate by Site-Directed Mutant Enzymes. The calculated steady-state turnover times for the S112A and H265A mutants ($t_{1/2} > 10$ min) were sufficiently high that enzyme-bound intermediates might be directly observable by NMR spectroscopy. Preliminary experiments indicated that turnover of a sample of 10 mM ^{13}C-labeled substrate to product by S112A and H265A mutant enzymes could be monitored on a time scale of several hours by ^{13}C NMR spectroscopy at 500 MHz, using a cryoprobe to record spectra (using 64 or 128 scans) in 5−10 min, thereby giving a number of "snapshots" of the enzyme-catalyzed reaction. The turnover at a substrate concentration of 10 mM is slower than predicted from k_{cat}, due to a certain amount of substrate inhibition, observed previously for *E. coli* MhpC (*7*).

An incubation of 1.0 mM H265A BphD with 10 mM ^{13}C-labeled substrate in 50 mM potassium phosphate buffer (pH 7.0) containing 10% D_2O was monitored directly by ^{13}C NMR spectroscopy at 298 K. The spectra are shown in Figure 2. In the first spectrum, obtained after 5 min, a new, line-broadened peak was observed at 128 ppm, in addition to the peak for the substrate (**1**) at 194 ppm. Over a period of 4 h, a series of four other spectra were recorded. In each spectrum, the broad peak at 128 ppm was maintained, and a sharp peak due to the product, benzoic acid (**5**), became gradually more prominent at 176 ppm. After 24 h at 298 K, the product peak had increased in size, and the peak at 128 ppm was still visible. A control experiment with enzyme only showed small envelopes at 170−175 and 120−130 ppm, due to amide carbonyl resonances and aromatic amino acids, respectively; the peak area of the envelope at 120−130 ppm is considerably smaller than the area of the new peak observed at 128 ppm.

The experiment was repeated with the S112A BphD mutant, and the spectra are shown in Figure 3. A similar broad peak at 128 ppm was observed in the first spectrum recorded after 10 min and in subsequent spectra up to 2.5 h, with the gradual appearance of the product signal at 176 ppm, at a rate similar to that of the H265A mutant. After 24 h at 298 K, the magnitude of the product peak had increased and it was more prominent than the substrate peak at 194 ppm, while the broad peak at 128 ppm was still visible. A control experiment with enzyme only yielded weak envelopes at 170−175 and 120−130 ppm.

Estimation of the expected chemical shift for the putative *gem*-diol intermediate (**4**) in the BphD reaction was carried out, using HIPPO-CNMRS software for ^{13}C chemical shift prediction (*27*). Using the *gem*-diol form of phenyl vinyl ketone as a model, a chemical shift of 122.3 ppm was predicted, indicating that the observed peak at 128 ppm is in the correct chemical shift range for the putative *gem*-diol intermediate.

An analysis of the line widths of the observed peaks was carried out, as shown in Figure 4. Immediately after mixing had taken place, the interaction of the substrate with the enzyme was witnessed by a pronounced broadening ($\eta_{1/2}$ increases from 15 to 55 Hz) and a slight upfield shift (ca 1.5 ppm) of the substrate resonance (see Figure 4A). The lack of a signal for free substrate indicates that free and bound substrate are in fast exchange relative to the NMR time scale, consistent with reversible binding (*16*). Close inspection of the substrate resonance at 194.5 ppm reveals that it consists of two signals. This might indicate the presence of two different enzyme-bound species, most likely the enol and keto tautomers. The line width of the resonance at 128 ppm in the presence of enzyme (see Figure 4B) is dramatically increased ($\eta_{1/2} \sim 200$ Hz), suggesting that this compound is interacting with the enzyme. Increased line widths are expected for protein-bound species, due to the slower molecular tumbling, and hence longer rotational

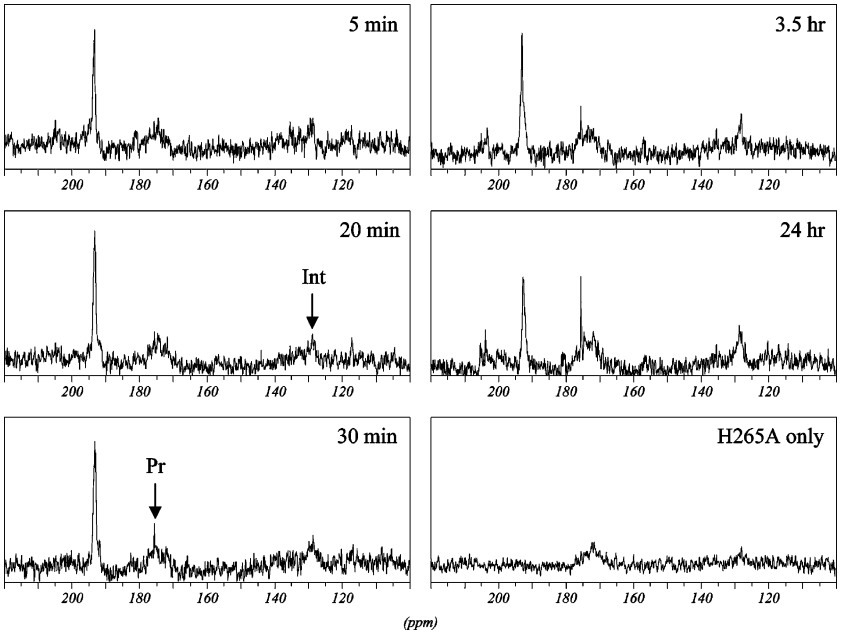

FIGURE 2: ^{13}C NMR spectra obtained for processing of ^{13}C-labeled substrate by the H265A BphD mutant. Spectra were recorded after 5 min, 20 min, 30 min, 3.5 h, and 24 h. The control spectrum of the H265A mutant enzyme only is shown in the final panel. Int, intermediate peak observed at 128 ppm; Pr, product peak at 176 ppm.

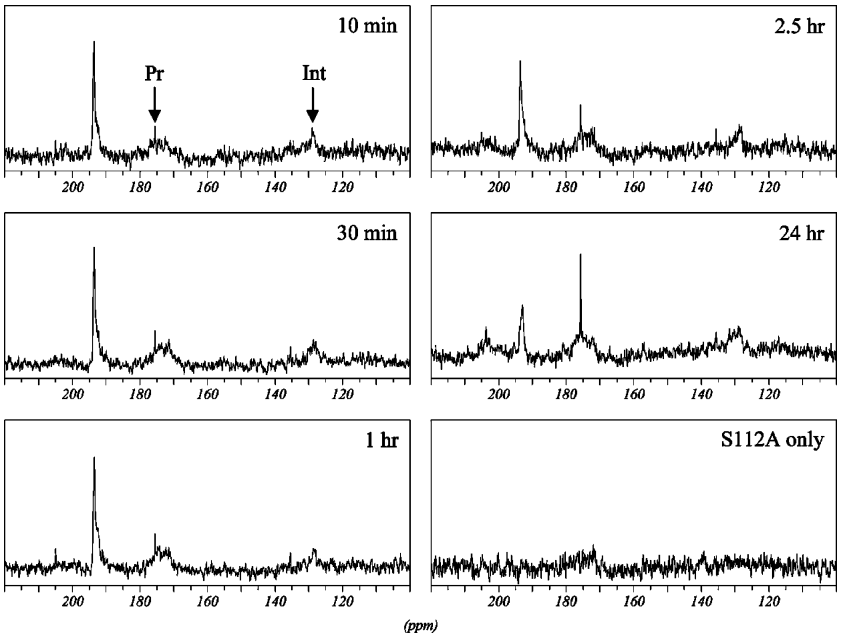

FIGURE 3: ^{13}C NMR spectra obtained for processing of ^{13}C-labeled substrate by the S112A BphD mutant. Spectra were recorded after 10 min, 30 min, 1 h, 2.5 h, and 24 h. The control spectrum of the S112A mutant enzyme only is shown in the final panel. Int, intermediate peak observed at 128 ppm; Pr, product peak at 176 ppm.

correlation times and transverse relaxation times in large molecules (*16*). Furthermore, exchange between bound and unbound species can also lead to line broadening (*16*), as exemplified by the resonances for the substrate. In contrast, the narrow line width of the product peak (5 Hz) suggests that the product, once formed, does not interact with the protein.

The same experiment was also carried out on a H114A mutant of C−C hydrolase MhpC, which has been shown previously to process the aryl-containing substrate with a low catalytic efficiency ($k_{cat} = 0.019$ s^{-1}) (*12*). The spectra are shown in Figure 5. In this case, after 10 min, approximately 90% conversion of substrate to product was observed, and once again, a peak was observed at 128 ppm. Continued monitoring of this experiment indicated that, following complete consumption of the substrate peak at 194 ppm, the intermediate peak at 128 ppm diminished somewhat in intensity but that a residual sharp doublet remained at 128 ppm, which was still present after 2.5 h.

A spectrum of ^{13}C-labeled substrate only, in the same buffer, showed a large peak at 194 ppm for the dienol substrate and also showed two small, sharp peaks ($\eta_{1/2} = 4$ Hz) at 128−130 ppm, similar in appearance to the residual signal described above. To ascertain whether the residual sharp doublet at 128 ppm was due to enzyme-bound material or a substrate decomposition product, a further control

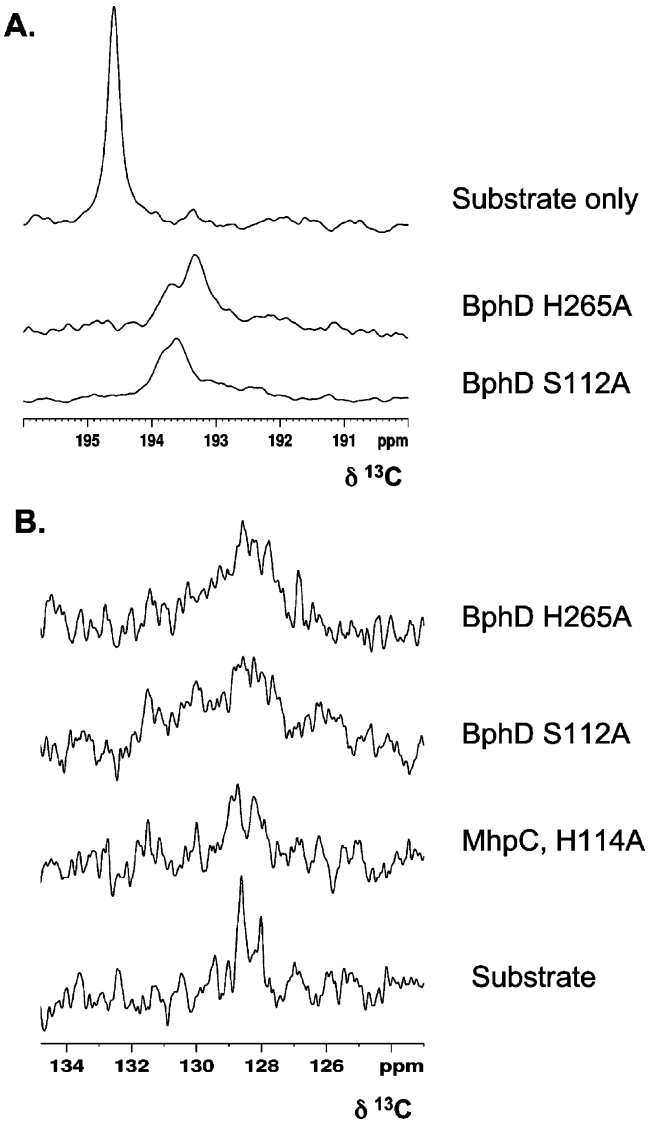

FIGURE 4: Analysis of line widths for (A) the substrate peak at 194 ppm, for the substrate-only control, and in presence of the H265A or S112A BphD mutant (10 min after mixing) and (B) the intermediate peak at 128 ppm, for the H265A BphD mutant (spectrum after a 20 min incubation), the S112A BphD mutant (spectrum after 30 min), the H114A MhpC mutant (spectrum after 30 min), and substrate only.

experiment in which an incubation of the enzyme with ^{13}C-labeled substrate was followed by addition of unlabeled substrate was carried out. The spectra are shown in Figure 6. The ^{13}C-labeled substrate (10 mM) was again mixed with a sample of H114A MhpC (1.0 mM), generating a broad peak at 128 ppm after 10 min, followed by a sharper peak at 128 ppm after 30 min. At this point, unlabeled substrate was added, at a final concentration of 20 mM. Further spectra were recorded, which still showed the presence of the sharp doublet at 128 ppm, indicating that the residual sharp doublet was not due to reversibly enzyme-bound material.

The observation of a similar sharp doublet in the substrate-only control experiment suggested that some nonenzymatic decomposition of the dienol substrate was occurring over the time scale of this experiment. Monitoring of the visible chromophore of the substrate at 434 nm versus time (see Figure 7A) shows that decomposition of the dienol substrate does occur, with a half-life of approximately 18 h in 50 mM potassium phosphate (pH 7.0). Analysis of a sample of ^{13}C-labeled substrate in buffer after 30 min by C_{18} reverse phase HPLC showed, in addition to the dienol substrate (retention time of 5 min), the formation of a new less polar species (retention time of 26.5 min). Analysis of the latter species by negative ion electrospray mass spectrometry gave an ion at *m*/*z* 218.27, indicating that it is isomeric with the substrate (expected M^+ 219.21). It is well-known that muconic acids readily lactonize in aqueous and nonaqueous solutions (*17*); therefore, we propose that this less polar, isomeric species is γ-lactone **6** formed by intramolecular cyclization, as shown in Figure 7B. Monitoring of substrate decomposition by ^{1}H NMR spectroscopy shows the formation of new peaks at 6.35 and 5.22 ppm, similar to the H-3 and H-4 protons of 2-keto-4-methyl-γ-butyrolactone (δ_H 6.22, 5.07), which exists as a mixture of enol and keto forms in aqueous solution (*18*). Hydration of the C-6 ketone of γ-lactone **6** would form *gem*-diol species **7a** and **7b**, shown in Figure 7B, with chemical shifts similar to those of *gem*-diol intermediate **4** in the BphD- and MhpC-catalyzed reactions, accounting for the presence of a residual sharp doublet in the experiments described above. Additional peaks at 200−205 ppm, corresponding to the keto form (**6**) of this γ-lactone, were also observed at longer reaction times in these experiments.

DISCUSSION

^{13}C NMR spectroscopy has been used previously to observe directly enzyme-bound intermediates such as the acyl−enzyme intermediate in the serine protease trypsin (*19*) and the acyl−enzyme thioester in the cysteine protease papain (*20*). The availability of specifically ^{13}C-labeled substrate for C−C hydrolase BphD, and 20−50 mg quantities of mutant enzymes with reduced k_{cat} values, has enabled us to investigate the existence of a *gem*-diol intermediate directly.

Replacement of Ser-112 or His-265 in *B. xenovorans* LB400 with Ala results in a 7000- or 4000-fold reduction in k_{cat}, respectively, similar in magnitude to the changes in k_{cat} observed in *E. coli* MhpC (*12*). Interpretation of pre-steady-state kinetic data for the S112A mutant indicates a fast initial ketonization step, but slow C−C cleavage, whereas in the H265A mutant, both steps are slow. This difference in kinetic behavior could explain the appearance of the enzyme-bound substrate peak by ^{13}C NMR (see Figure 4A). In the H265A mutant, two signals are observed, corresponding to bound dienol and keto isomers, whereas in the S112A mutant, a single peak is observed, since the bound dienol is rapidly converted to the keto tautomer. In each case, pre-steady-state kinetic analysis establishes that the C−C cleavage step is rate-limiting.

Upon incubation of a 10-fold excess of 6-^{13}C-labeled substrate with the S112A or H265A BphD mutant, or with the H114A MhpC mutant, a broad peak was observed at 128 ppm during steady-state turnover, on the same time scale as the conversion of substrate to product. Literature chemical shift values for alkyl *gem*-diols are typically in the range of 90−100 ppm; for example, an intermediate observed by ^{13}C NMR spectroscopy in the binding of a pepstatin analogue to pepsin was observed at 99 ppm (*21*). However, the putative *gem*-diol intermediate in the BphD reaction is adjacent to

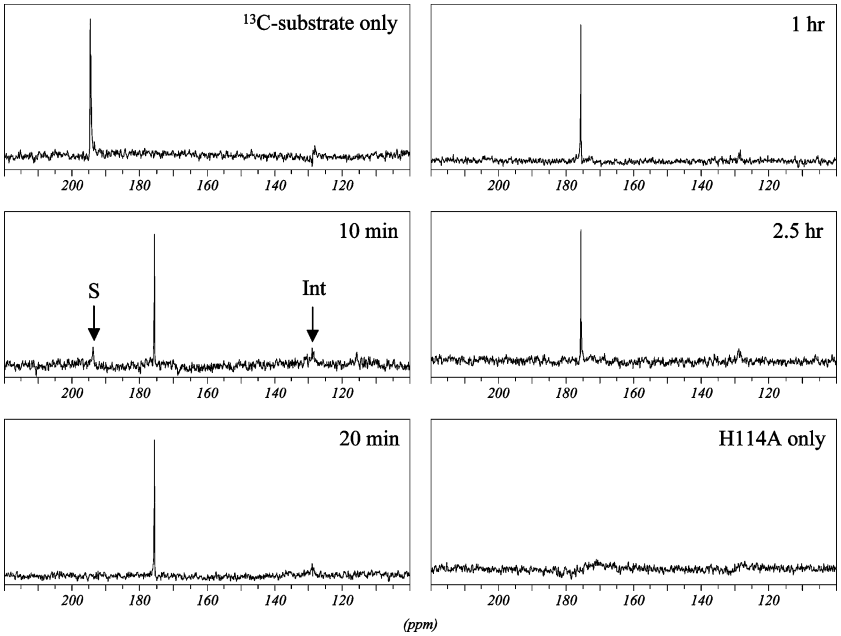

FIGURE 5: ^{13}C NMR spectra obtained for processing of ^{13}C-labeled substrate by the H114A MhpC mutant. Spectra were recorded after 10 min, 20 min, 1 h, and 2.5 h. The spectrum of the ^{13}C-labeled substrate only is shown in the first panel; the spectrum of the H114A mutant enzyme only is shown in the final panel. Int, intermediate peak observed at 128 ppm; S, substrate peak at 194 ppm.

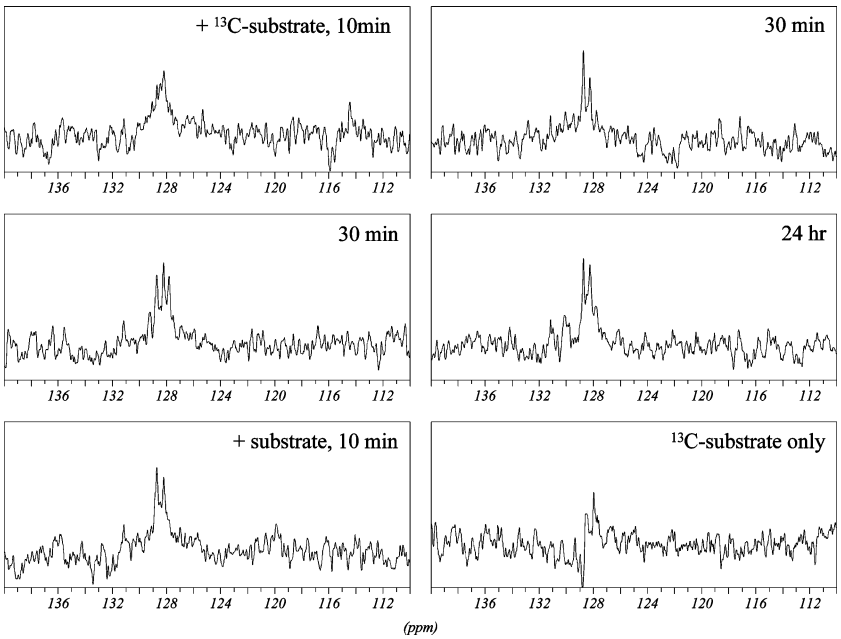

FIGURE 6: ^{13}C NMR spectra obtained for processing of ^{13}C-labeled substrate followed by unlabeled substrate by the H114A MhpC mutant, showing the 110−140 ppm region of the spectrum: enzyme with ^{13}C-labeled substrate after 10 and 30 min, unlabeled substrate added after a further 10 min, 30 min, or 24 h. The final panel shows ^{13}C-labeled substrate only, in the same region.

an aromatic ring, which will cause a downfield chemical shift. Synthetic ethylenedioxy ketals of the aryl substrate synthesized previously (*8*) gave ^{13}C signals at 107−108 ppm, and the unalkylated *gem*-diol would be expected at a 15−20 ppm higher chemical shift. Moreover, chemical shift estimation using the HIPPO-CNMRS prediction software, using the *gem*-diol of phenyl vinyl ketone as a model, gives an estimate of 122.3 ppm (*27*). Therefore, the broad peak observed at 128 ppm is at an expected chemical shift for a *gem*-diol, whereas an acyl−enzyme intermediate would be expected at ∼170−175 ppm (*15*).

The possibility that this species is a hemi-ketal adduct arising from nucleophilic attack of Ser-112 is considered very unlikely, for the following reasons. (1) This species is also observed in the S112A mutant, which would be unable to form such an adduct. (2) Formation of such a hemi-ketal would be immediately followed by formation of an acyl enzyme (**3**), which is not observed.

If the observed peak corresponds to a catalytic intermediate, then it should disappear at the end of the reaction, after substrate turnover is completed. In the case of the H265A and S112A mutant BphD enzymes, turnover was still incomplete after 24 h; however, in the case of the H114A MhpC mutant, turnover was complete after 10−15 min. The presence of a residual sharp doublet at 128 ppm at longer reaction times in this experiment, also observed in the

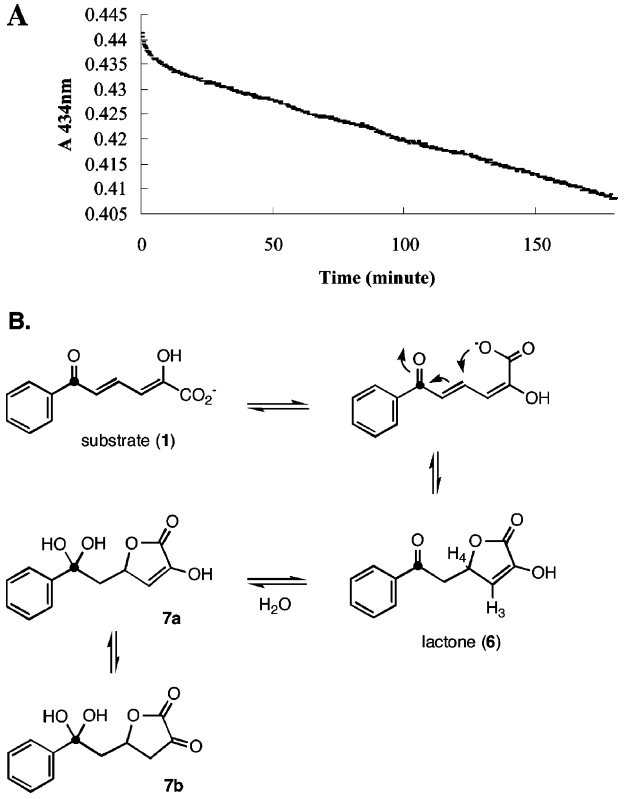

FIGURE 7: Nonenzymatic decomposition of the dienol substrate. (A) Decomposition of 33 μM substrate in 50 mM potassium phosphate buffer (pH 7.0) at 25 °C. (B) Scheme illustrating intramolecular cyclization of substrate to form the γ-lactone by the product.

substrate-only control experiment, prompted us to examine closely the line widths of the relevant peaks and carry out further control experiments. The line width of the broad peak formed during turnover, at ~200 Hz, is much greater than that of the doublet observed at longer times in the H114A mutant (5 Hz) and in the substrate-only control (4 Hz). Furthermore, the residual doublet in the H114A mutant is not removed upon treatment with excess unlabeled substrate. These data imply that the broad peak is an enzyme-bound species, whereas the sharp signals are due to solution species.

We have further investigated the nonenzymatic decomposition of the substrate, which undergoes an intramolecular lactonization reaction on a similar time scale, generating a γ-lactone (**6**) containing an aryl ketone, which will in aqueous solution hydrate to form *gem*-diol contaminants **7a** and **7b**, as shown in Figure 7B. We therefore conclude that the broad peak observed at 128 ppm in H265A and S110A mutants of BphD and the H114A mutant of MhpC is the proposed *gem*-diol reaction intermediate (*4*), arising from base-catalyzed attack of water upon a ketonized substrate. This experiment provides further evidence that the catalytic serine residue in the C−C hydrolase enzymes does not act as a nucleophile during the catalytic mechanism.

A non-nucleophilic role for the serine catalytic triad, also proposed by Kratky et al. for *Hevea brasiliensis* hydroxynitrile lyase on the basis of crystallographic studies (*22*), is a significant departure from the nucleophilic mechanism of the serine proteases and implies that alternative general base mechanisms are possible for other α/β-hydrolase enzymes. It is interesting to note that general base mechanisms have also been implicated in two C−C hydrolases of different structural classes: human fumarylacetoacetate hydrolase (*23*) and *Rhodococcus* 6-oxocamphor hydrolase (*24*). In each of these enzymes, a histidine active site base has been identified, found as a dyad with a Glu and an Asp residue, respectively. A His/Asp dyad is also involved in a general base mechanism in phospholipase A2 (*25*). The His/Asp dyad is therefore used in several enzymes for general base catalysis of addition of water to a carbonyl substrate, forming an oxyanion intermediate. In MhpC and BphD, the active site serine residue appears to have an important role in stabilizing the oxyanion intermediate that is formed, whereas in fumarylacetoacetate hydrolase, nearby Arg-237 and Gln-240 appear to carry out oxyanion stabilization (*23*).

ACKNOWLEDGMENT

We thank Andrew Mason, Peter Grice (University of Cambridge, Cambridge, U.K.), and Adam Clarke (University of Warwick, Coventry, U.K.) for assistance with NMR spectroscopy.

REFERENCES

1. Heikinheimo, P., Goldman, A., Jeffries, C., and Ollis, D. L. (1999) Of barn owls and bankers: A lush variety of α/β hydrolases, *Structure 7*, R141−R146.
2. Schrag, J. D., and Cygler, M. (1997) Lipases and the α/β hydrolase fold, *Methods Enzymol. 284*, 85−107.
3. Bugg, T. D. H. (2004) Diverse catalytic activities in the $\alpha\beta$-hydrolase family: Activation of H_2O, H_2O_2, HCN, and O_2, *Bioorg. Chem. 32*, 367−375.
4. Bugg, T. D. H., and Winfield, C. J. (1998) Enzymatic cleavage of aromatic rings: Mechanistic aspects of the catechol dioxygenases and later enzymes of bacterial oxidative cleavage pathways, *Nat. Prod. Rep. 15*, 513−530.
5. Lam, W. W. Y., and Bugg, T. D. H. (1997) Purification, characterisation and stereochemical analysis of a C-C hydrolase: 2-Hydroxy-6-keto-nona-2,4-diene 1,9-dioic acid 5,6-hydrolase, *Biochemistry 36*, 12242−12251.
6. Henderson, I. M. J., and Bugg, T. D. H. (1997) Pre-steady state kinetic analysis of 2-hydroxy-6-keto-nona-2,4-diene 1,9-dioic acid 5,6-hydrolase: Kinetic evidence for enol/keto tautomerisation, *Biochemistry 36*, 12252−12258.
7. Fleming, S. M., Robertson, T. A., Langley, G. J., and Bugg, T. D. H. (2000) Catalytic mechanism of a C-C Hydrolase enzyme: Evidence for a *gem*-diol intermediate, not an acyl enzyme, *Biochemistry 39*, 1522−1531.
8. Speare, D. M., Fleming, S. M., Beckett, M. N., Li, J.-J., and Bugg, T. D. H. (2004) Synthetic 6-aryl 2-hydroxy-6-keto-hexa-2,4-dienoic acid substrates for C-C hydrolase BphD: Investigation of a general base catalytic mechanism, *Org. Biomol. Chem. 2*, 2942−2950.
9. Nandhagopal, N., Yamada, A., Hatta, T., Masai, E., Fukuda, M., Mitsui, Y., and Senda, T. (2001) Crystal structure of 2-hydroxyl-6-oxo-6-phenylhexa-2,4-dienoic acid (HPDA) hydrolase (BphD) from the *Rhodococcus* sp. strain RHA1 of the PCB degradation pathway, *J. Mol. Biol. 309*, 1139−1151.
10. Fushinobu, S., Saku, T., Hidaka, M., Jun, S.-Y., Nojiri, H., Yamane, H., Shoun, H., Omori, T., and Wakagi, T. (2002) Crystal structures of a *meta*-cleavage product hydrolase from *Pseudomonas fluorescens* IP01 (CumD) complexed with cleavage products, *Protein Sci. 11*, 2184−2195.
11. Dunn, G., Montgomery, M. G., Mohammed, F., Coker, A., Cooper, J. B., Robertson, T., Garcia, J.-L., Bugg, T. D. H., and Wood, S. P. (2005) The structure of the C-C bond hydrolase MhpC provides insights into its catalytic mechanism, *J. Mol. Biol. 346*, 253−265.
12. Li, C., Montgomery, M. G., Mohammed, F., Li, J.-J., Wood, S. P., and Bugg, T. D. H. (2005) Catalytic mechanism of C-C hydrolase MhpC: Elucidation of the roles of His-263 and Ser-

110 from kinetic analysis of site-directed mutant enzymes, *J. Mol. Biol. 346*, 241−251.
13. Seah, S. Y. K., Terracina, G., Bolin, J. T., Riebel, P., Snieckus, V., and Eltis, L. D. (1998) Purification and preliminary characterisation of a serine hydrolase involved in the microbial degradation of polychlorinated biphenyls, *J. Biol. Chem. 273*, 22943−22949.
14. Speare, D. M., Olf, P., and Bugg, T. D. H. (2002) Hammett analysis of a C-C hydrolase-catalysed reaction using synthetic 6-aryl 2-hydroxy-6-keto-hexa-2,4-dienoic acid substrates, *J. Chem. Soc., Chem. Commun.*, 2304−2305.
15. Li, J.-J., and Bugg, T. D. H. (2005) Stereochemistry of the reaction catalysed by 2-hydroxy-6-keto-6-phenyl-hexa-2,4-dienoic acid 5,6-hydrolase (BphD), *Chem. Commun.*, 130−132.
16. London, R. E. (1993) Chemical-shift and linewidth characteristics of reversibly bound ligands, *J. Mag. Reson., Ser. A 104*, 190−196.
17. Weller, M. G., and Weser, U. (1982) Ferric nitrilotriacetate: An active center analog of pyrocatechase, *J. Am. Chem. Soc. 104*, 3752−3754.
18. Pollard, J. R., and Bugg, T. D. H. (1998) Purification, characterisation and reaction mechanism of monofunctional 2-hydroxypentadienoic acid hydratase from *Escherichia coli*, *Eur. J. Biochem. 251*, 98−106.
19. Mackenzie, N. E., Malthouse, J. P. G., and Scott, A. I. (1984) Cryoenzymology of trypsin: ^{13}C-NMR detection of an acyl-trypsin intermediate in the trypsin-catalysed hydrolysis of a highly specific substrate at sub-zero temperature, *Biochem. J. 219*, 437−444.
20. Malthouse, J. P. G., Gamcsik, M. P., Boyd, A. S. F., Mackenzie, N. E., and Scott, A. I. (1982) Croenzymology of proteases: NMR detection of a productive thioacyl derivative of papain at subzero temperature, *J. Am. Chem. Soc. 104*, 6811−6813.
21. Rich, D. H., Bernatowicz, M. S., and Schmidt, P. G. (1982) Direct ^{13}C NMR evidence for a tetrahedral intermediate in the binding of a pepstatin analogue to porcine pepsin, *J. Am. Chem. Soc. 104*, 3535−3536.
22. Zuegg, J., Gruber, K., Gugganig, M., Wagner, U. G., and Kratky, C. (1999) Three-dimensional structure of enzyme-substrate complexes of the hydroxynitrile lyase from *Hevea brasiliensis*, *Protein Sci. 8*, 1990−2000.
23. Bateman, R. L., Bhanumoorthy, P., Witte, J. F., McClard, R. W., Grompe, M., and Timm, D. E. (2001) Mechanistic inferences from the crystal structure of fumarylacetoacetate hydrolase with a bound phophorus-based inhibitor, *J. Biol. Chem. 276*, 15284−15291.
24. Leonard, P. M., and Grogan, G. (2004) Structure of 6-oxo camphor hydrolase H122A mutant bound to its natural product (2*S*,4*S*)-α-campholinic acid, *J. Biol. Chem. 279*, 31312−31317.
25. Dessen, A. (2000) Structure and mechanism of human cytosolic phospholipase A_2, *Biochim. Biophys. Acta 1488*, 40−47.
26. Ho, S. N., Hunt, H. D., Horton, R. M., Pullen, J. K., and Pease, L. R. (1989) Site-directed mutagenesis by overlap extension using the polymerase chain reaction, *Gene 77*, 51−59.
27. Hönig, H. (1997) HIPPO-CNMRS: Highly improved prediction program of carbon nuclear magnetic resonance shifts, *J. Chem. Educ. 4D*, 15−16.

BI0612519